Chemical Engineering Journal 489 (2024) 151447

Contents lists available at ScienceDirect

Chemical Engineering Journal

journal homepage: www.elsevier.com/locate/cej

Polymerizable deep eutectic solvents: Convenient reactive dispersion media for the preparation of novel multi-walled carbon nanotubes-based functional materials

Laura Valentino [a], Riccardo Di Forti [a], Anthony Morena [b], Carmela Aprile [b], Michelangelo Gruttadauria [a,*], Francesco Giacalone [a,*], Vincenzo Campisciano [a,*]

[a] Department of Biological, Chemical and Pharmaceutical Sciences and Technologies, University of Palermo and INSTM UdR Palermo, Viale Delle Scienze, Ed. 17 90128, Palermo Italy

[b] Laboratory of Applied Material Chemistry (CMA), Department of Chemistry, NISM, University of Namur, 61 rue de Bruxelles 5000, Namur Belgium

ARTICLE INFO

Keywords:
Deep Eutectic Solvents
Polymerization
Carbon Nanotubes
Ionic Liquids
CO_2 conversion

ABSTRACT

A new straightforward and green approach for the covalent functionalization of multi-walled carbon nanotubes (MWCNTs) was developed. This carbon nanostructure was efficiently derivatized by polymerizing proper deep eutectic monomers (DEM), a subclass of deep eutectic solvents (DES), based on a series of mono- and bis-vinyl imidazolium salts endowed with different functional groups (–OH, $–NH_2$, $–NH_3^+Br^-$) in the side chain or in the spacer. Herein, DEM systems played a triple role as convenient dispersion media for MWCNTs, efficient reactive systems, and also as structure-directing agents for the radical-initiated polymerization process onto the surface of MWCNTs. In addition, the new methodology allowed obtaining highly functionalized hybrid materials, as shown by thermogravimetric analyses, in short reaction times (<1h). Transmission electron microscopy (TEM) revealed that the polymeric network orderly develops along the surface of the nanotubes, which act as templating agent for both mono- and bis-vinyl imidazolium salts, despite the random nature of the polymerization process for the latter species. This new functionalization strategy of MWCNTs stands out for its environmentally friendly and time-saving nature leading to the formation of materials with significant potential for applications in a plethora of research fields. As a proof of their possible application, we tested these new hybrid materials as recoverable and recyclable catalysts for the conversion of CO_2 into cyclic carbonates under solvent-free conditions, showing good catalytic performances, even in the absence of additional co-catalysts.

1. Introduction

In the field of nanomaterials science and nanotechnology, multi-walled carbon nanotubes (MWCNTs) are gaining increasing importance due to their adaptability to meet specific requirements for various applications [1–4]. The remarkable electronic, mechanical, and thermal properties exhibited by this allotropic form of carbon make them highly desirable materials in a wide range of application fields, including energy conversion and storage, electronics, catalysis, optoelectronics, sensing, drug delivery systems, biomedicine, and the formation of high-performance materials such as films and fibers [5–12].

Despite their outstanding properties, carbon nanotubes usually exhibit poor dispersibility in common solvents. Indeed, pristine CNTs typically aggregate in bundles due to van der Waals and π–π stacking interactions between the tube walls. This results in the formation of highly entangled 3D networks that make it difficult to achieve stable and fine dispersions in both aqueous and organic media, limiting their potential.

To enhance the dispersibility of CNTs and broaden their potential applications, a key strategy involves chemical modifications of their structures [13,14]. Chemical surface functionalization has the dual purpose of preventing nanotubes aggregation and promoting the synthesis of innovative materials in which the intrinsic properties of CNTs are combined with those of the functionalization units, resulting in hybrid systems with vast potential for various applications. One way to obtain the chemical modification of CNTs is represented by the use of

* Corresponding authors.
E-mail addresses: michelangelo.gruttadauria@unipa.it (M. Gruttadauria), francesco.giacalone@unipa.it (F. Giacalone), vincenzo.campisciano@unipa.it (V. Campisciano).

https://doi.org/10.1016/j.cej.2024.151447
Received 13 February 2024; Received in revised form 15 April 2024; Accepted 17 April 2024
Available online 18 April 2024

corrosive acids, oxidizing agents, and/or other hazardous chemicals often leading to the permanent deep damage of the sidewalls of carbon nanotubes [14–16].

An alternative method is represented by non-covalent interactions of CNTs with suitable dispersing agents. In this context, in 2003, Fukushima et *al.* discovered that when mixed with imidazolium-based ionic liquids (ILs), pristine carbon nanotubes gave rise to physical gel, the so-called bucky gels [17,18]. The mere combination of ILs with carbon nanotubes resulted in the dispersion and separation of the entangled nanotubes. The excellent processability of pristine CNTs within these gels was attributed to a sort of shielding effect that ILs, with their high dielectric constants, exert onto the strong π–π stacking interaction among CNTs [19].

ILs can be deemed inherently superior to conventional organic solvents for dispersing CNTs owing to their characteristics, such as reduced flammability, minimal or absent volatility, exceptional thermal stability, and notable ionic conductivity. Moreover, the unique interactions between ILs and nanocarbons confer distinctive properties to these nanocomposites, improving their dispersibility in various environments and expanding their field of use [18,20,21].

ILs have also been used for the covalent modification of the surface of carbon nanoforms (CNFs) such as single- and multi-walled carbon nanotubes and carbon nanohorns. In particular, different bis-vinyl imidazolium salts have been exploited to achieve CNFs-functionalization with highly cross-linked polymer networks, through a radical polymerization process. More in depth, a good degree of functionalization variability was explored by changing the identity of the spacer and/or the anion [22–25] or by co-polymerizing bis-vinyl imidazolium salts with different vinyl building block species [26,27].

Another viable alternative for achieving optimal results in nanotube dispersion involves the use of a class of solvents that shares some of the advantageous characteristics of ILs, the deep eutectic solvents (DESs). [28–31] These eutectic mixtures have gained significant interest over the last twenty years as a new category of environment friendly solvents [32]. Their minimal toxicity, biodegradability, ease of synthesis, and low cost makes them desirable in the large-scale synthesis of novel functional materials. This heightened attention follows a study by Abbott et *al.*, [33,34] who observed an unusually pronounced reduction in melting point of the eutectic mixture of specific hydrogen bond donors (HBDs) and acceptors (HBAs) with respect to the parent compounds. In addition, they can be tailored to meet specific features by selecting appropriate components and adjusting their molar ratio, making them versatile and promising in a wide range of applications [35]. However, the role of DESs is not only limited to that of a green reaction medium for CNTs dispersion, and in this context, interesting examples are reported by Gutiérrez and co-workers, who have successfully used DESs, containing CNTs in suspension, for the dissolution of polymerizable monomer/s (furfuryl alcohol or resorcinol–formaldehyde pair) for nanocomposite preparation [36–39]. However, DESs can express greater potential, in fact, if one component of the DES is involved in the functionalization of the carbon nanostructure, then DES can act as both dispersion medium of CNTs and reactant [40].

Specifically, this particular class of deep eutectic solvents, characterized by the inclusion of polymerizable units within either HBD or HBA components has been pioneered and defined as deep eutectic monomers (DEMs) by Mota-Morales et *al.*, who applied the so-called frontal polymerization in DESs by employing combinations of "classic monomers" such as acrylic acid or methacrylic acid with choline chloride [41]. These DEMs were characterized by the inclusion of a polymerizable acrylate group within the hydrogen bond donor unit. Furthermore, they explored the frontal polymerization using DEMs consisting of various ammonium salts and hydrogen bond donors containing acrylic acids and acrylamides [42]. DEMs can represent a very intriguing solution to reduce the dependence on classical volatile organic solvents in the production of polymers. The high flexibility in the DEMs formation by changing both the nature and the molar ratio of the constituent species close to the eutectic point to meet specific requirements allow to expand the conditions in which polymerization takes place.

In the light of the above, the advantageous features of DEMs pave the way for the optimization of a convenient methodology for covalent anchoring of the polymerizable component of DEM onto the CNTs surface with the production of novel functional materials. However, during the polymerization process, the depletion of the polymerizable component of the DEM, causes the change of the starting HBD/HBA molar ratio inducing the eutectic rupture and a phase segregation by means of a spinodal decomposition and the formation of a polymer-depleted solid phase, mainly consisting of the inert component of the DEM [43,44]. The formation of this solid phase could have significant consequences on the morphology of the resulting material.

However, although some alkyl imidazolium salts as HBA have been used to obtain a classic DES system, [45–51] conversely, to date no imidazolium salts with mono- or bis-vinyl moieties used as polymerizable HBA have been employed in the formation of DEMs. Therefore, herein, a new synthetic method employing deep eutectic monomers as environmentally friendly reaction media and reactive agents for the functionalization of MWCNTs is reported. In particular, the radical polymerization of mono- or bis-vinyl imidazolium salts, used for the first time as HBA components of DEMs systems, in the presence of CNTs structures was investigated. Interestingly, the CNTs outer walls acted as template for the growth of highly compact polymeric imidazolium networks for both mono- and bis-vinyl imidazolium salts, despite the random nature of the polymerization process. The resulting materials were employed as heterogeneous and recyclable catalysts for the conversion of CO_2 and epoxides to generate cyclic carbonates.

2. Experimental section

2.1. Materials and methods

Chemicals and solvents were purchased from commercial suppliers and used without further purification. Thermogravimetric analysis (TGA) was performed in a Mettler Toledo TGA STAR system with a heating rate of 10 °C/min, either under oxygen flow from 100 to 1000 °C or under nitrogen flow from 25 to 900 °C. Differential scanning calorimetry (DSC) measurements were carried out with a TA Instruments mod. 2920 differential scanning calorimeter (TA Instrument Inc., New Castle, DE, USA) equipped with a TA Instruments refrigerated cooling system. Samples (~4 mg) were weighed in aluminium TA Tzero hermetic pans, which were subsequently sealed with aluminium lids. The analyses were performed with heating and cooling rates of 10 °C min^{-1} under a N_2 atmosphere of 60 mL min^{-1}. Raman spectra were acquired using Horiba LabRam HR Evolution equipment with a 532 nm laser line, using a spectral resolution of about 7 cm^{-1} and a laser intensity that does not interfere with the signal. Transmission electron microscopy (TEM) images were recorded using a Philips Tecnai 10 microscope operating at 80–100 kV. Nitrogen adsorption–desorption analyses were carried out at 77 K in a Micromeritics ASAP 2420 volumetric adsorption analyzer. Before the analysis the sample was pre-treated at 150 °C for 8 h under reduced pressure (0.1 mbar). The Brunauer-Emmett-Teller (BET) method was applied in the 0.05–0.30p/p_0 range to calculate the specific surface area, whereas the pore size distributions were estimated from the adsorption isotherm using the BJH method. ^{1}H NMR spectra were recorded on a Bruker 400 MHz spectrometer. Solid state ^{13}C NMR spectra were recorded at room temperature on a JEOL ECZ-R spectrometer operating at 11.7 T using a 3.2 mm AUTOMAS probe and spinning frequencies of 10 kHz. FT-IR measurements were performed in absorbance mode using a Perkin Elmer two DEP.

2.2. Synthetic procedures

2.2.1. Synthesis of 1-hydroxyethyl-3-vinyl imidazolium bromide (1a)

Compound **1a** was synthesized according to a previously reported procedure [52]. In a 50 mL two-neck round-bottom flask, 1-vinylimidazole (34.61 mmol, 3.2 mL), 2-bromoethanol (34.83 mmol, 2.6 mL), and 17.5 mL of ethanol were added. The mixture was stirred at 80 °C under an argon atmosphere for 48 h. After cooling down to room temperature, the solvent was removed under reduced pressure and the viscous residue was washed several times with diethyl ether until all the starting unreacted reagents were removed. Once dried at 40 °C under vacuum, a highly viscous yellow compound was obtained (6.6 g; 86 %). ^{1}H NMR (400 MHz, DMSO-D6, δ): 9.50 (s, 1H), 8.22 (s, 1H), 7.89 (s, 1H), 7.34 (dd, J = 15.7, 8.8 Hz, 1H), 5.98 (dd, J = 15.6, 2.3 Hz, 1H), 5.42 (dd, J = 8.7, 2.3 Hz, 1H), 4.39 – 4.17 (m, 2H), 3.91 – 3.66 (m, 2H); ^{13}C NMR (101 MHz, DMSO-D6, δ): 136.21, 129.36, 124.19, 119.33, 109.08, 59.61, 52.58.

2.2.2. Synthesis of 3-ammoniopropyl-1-vinyl imidazolium bromide (1b)

The synthesis of compound **1b** was carried out according to a previously reported procedure with minor changes [53]. A solution of 3-bromopropylamine hydrobromide (15.9 mmol, 3.55 g) and 1-vinylimidazole (15.9 mmol, 1,47 mL) in acetonitrile (7.95 mL) was heated at 75 °C, under stirring, for 24 h. After cooling down to room temperature, the solvent was removed under reduced pressure and the solid residue was washed several times with diethyl ether. The obtained white solid was dried under vacuum at 40 °C (4.72 g; 95 %). ^{1}H NMR (400 MHz, DMSO-D6, δ): 9.63 (s, 1H), 8.26 (s, 1H), 7.99 (s, 2H), 7.34 (dd, J = 15.6, 8.8 Hz, 1H), 5.99 (dd, J = 15.6, 2.0 Hz, 1H), 5.43 (dd, J = 8.7, 2.0 Hz, 1H), 4.35 (t, J = 6.8 Hz, 1H), 2.86 (d, J = 6.1 Hz, 2H), 2.27 – 1.78 (m, 2H). ^{13}C NMR (101 MHz, DMSO-D6, δ): 136.25, 129.51, 123.75, 119.81, 109.29, 46.93, 36.27, 27.82.

2.2.3. Synthesis of bis(vinyl)imidazolium bromide (1c)

The synthesis of compound **1c** was carried out according to a previously reported procedure [27]. A solution of 1-vinylimidazole (1.5 mL, 16 mmol) and 1,4-dibromobutane (950 μL, 7.88 mmol) in methanol (2 mL) was heated overnight at 65 °C, under stirring, in Ar atmosphere, and in the dark. After cooling down to room temperature, the solvent was removed under reduced pressure and the solid residue was washed several times with diethyl ether, until all the starting unreacted reagents were removed. The obtained white solid was dried under vacuum at 60 °C (3.1 g; 98 %). ^{1}H NMR (400 MHz, CD_3OD, δ): 9.41 (s, 1H), 8.01 (t, J = 1.8 Hz, 1H), 7.81 (d, J = 1.8 Hz, 1H), 7.26 (dd, J = 15.6, 8.7 Hz, 1H), 5.93 (dd, J = 15.6, 2.7 Hz, 1H), 5.44 (dd, J = 8.7, 2.7 Hz, 1H), 4.35 (t, J = 6.7 Hz, 2H), 2.02 (dd, J = 6.6, 3.4 Hz, 2H).^{13}C NMR (101 MHz, DMSO-D6, δ): 136.00, 129.42, 123.78, 119.69, 109.21, 48.91, 26.24.

2.2.4. Synthesis of 1,3-bis(3-vinylimidazolium)propan-2-ol bromide (1d)

The synthesis of compound **1d** was carried out according to a previously reported procedure [22]. A solution of 1,3-dibromopropan-2-ol (5 mmol, 1.09 g) and 1-vinylimidazole (16 mmol, 1.44 mL) in15 mL of acetonitrile was heated at 80 °C for 5 days, under stirring, in Ar atmosphere, and in the dark. After cooling down to room temperature, the solvent was removed under reduced pressure and the solid residue was washed several times with diethyl ether, until all the starting unreacted reagents were removed. The obtained white solid was dried under vacuum at 60 °C (1.967 g, 97 %). ^{1}H NMR (400 MHz, DMSO-D6, δ): 9.75 (s, 1H), 8.45 (s, 1H), 8.13 (s, 1H), 7.56 (dd, J = 15.7, 8.8 Hz, 1H), 6.19 (dd, J = 15.6, 2.4 Hz, 1H), 5.62 (dd, J = 8.8, 2.4 Hz, 1H), 4.69 (dd, J = 13.7, 3.0 Hz, 1H), 4.38 (dd, J = 13.7, 8.1 Hz, 1H), 3.66 – 3.44 (m, 1H).^{13}C NMR (101 MHz, DMSO-D6, δ): 136.56, 129.35, 124.47, 119.46, 109.38, 67.84, 52.67.

2.2.5. Synthesis of 1,3-bis(1-vinyl-imidazolium)(2,2-bis(hydroxymethyl) propane bromide (1e)

The synthesis of compound **1e** was obtained through the reaction between 2,2′-bisbromethyl-1,3-propanediol (3.74 mmol, 1 g) and 1-vinylimidazole (11.22 mmol, 1.02 mL) in DMF (1 mL). The mixture was heated at 120 °C for 120 h, under stirring, in Ar atmosphere, and in the dark. After 24 h, 1 mL of DMF was added to the mixture, and another 2 mL of DMF after further 48 h. After cooling down to room temperature, the solvent was removed under reduced pressure and the solid residue was washed several times with diethyl ether. Afterwards, the precipitate was transferred into a centrifuge tube and cold methanol (6 mL) was added. The tube was kept at −20 °C for 10 min before centrifugation (3 min, 3000 rpm). The operation was repeated twice with methanol and once with diethyl ether. The obtained brown solid was dried under vacuum at 60 °C (1.23 g; 73.2 %). ^{1}H NMR (400 MHz, DMSO-D6, δ): 9.51 (s, 1H), 8.31 (s, 1H), 7.84 (s, 1H), 7.38 (dd, J = 15.5, 8.7 Hz, 1H), 6.03 (dd, J = 15.6, 2.3 Hz, 1H), 5.46 (dd, J = 8.8, 2.2 Hz, 1H), 4.34 (s, 1H), 3.22 (s, 2H). ^{13}C NMR (101 MHz, DMSO-D6, δ): 136.75, 128.82, 124.78, 118.70, 108.82, 58.49, 49.18, 45.38.

2.2.6. General procedure for the synthesis of DEM systems (2a-e)

In a 5 mL glass vial, mono or bis-vinyl imidazolium salt **1a-e** (HBA) and urea or dimethylurea (HBD) were added in 1:2 or 1:4 ratio with respect to bromide ions. The two solid components were allowed to mix at 80 °C for 2 h, under stirring (500 rpm). HBA species **1a-c** always gave rise to homogeneous liquids when mixed in all investigated ratios with HBD species, namely urea or dimethylurea in the 1:2 and 1:4 ratios. In the case of HBA species **1d-e**, a homogeneous liquid was only formed using a 1:4 ratio with dimethylurea as HBD.

2.2.7. General procedure for the synthesis of hybrid materials (3a-e)

Once the DEM formed, MWCNTs were added and the mixture was heated at 80 °C for 30 min. AIBN was added under Ar atmosphere and the reaction mixture was allowed to react at 80 °C for 40 min. The obtained dark residue was transferred into a centrifuge tube and methanol was added. The residue was subjected to centrifugation and the supernatant was removed. The solid was further washed three times with methanol and once with diethyl ether. The washings were combined and dried under vacuum to recover the corresponding HBD. The residue was recovered and dried under vacuum at 40 °C.

2.2.8. Synthesis of hybrid material 3a

In a 5 mL glass vial, imidazolium salt **1a** (2 mmol, 438.1 mg) and urea (8 mmol, 485.3 mg) were added in 1:4 ratio with respect to bromide ions. The two solid components were allowed to mix at 80 °C for 2 h, under stirring (500 rpm). Once the DEM formed, MWCNTs (50 mg) were added and the mixture was heated at 80 °C for 30 min. AIBN (5 mol %, 18 mg) was added under Ar atmosphere and the reaction mixture was allowed to react at 80 °C for 40 min. The obtained dark residue was transferred into a centrifuge tube and methanol was added. The residue was subjected to centrifugation and the supernatant was removed. The solid was further washed with DMSO, methanol, and diethyl ether. The residue was recovered and dried under vacuum at 40 °C (450 mg; 92 %).

2.2.9. Synthesis of hybrid material 3b

In a 5 mL glass vial, imidazolium salt **1b** (1 mmol, 313 mg) and urea (4 mmol, 240 mg) were added in 1:2 ratio with respect to bromide ions. The two solid components were allowed to mix at 80 °C for 2 h, under stirring (500 rpm). Once the DEM formed, MWCNTs (25 mg) were added and the mixture was heated at 80 °C for 30 min. AIBN (5 mol%, 9 mg) was added under Ar atmosphere and the reaction mixture was allowed to react at 80 °C for 40 min. The obtained dark residue was transferred into a centrifuge tube and methanol was added. The residue was subjected to centrifugation and the supernatant was removed. The solid was further washed with DMSO, methanol, and diethyl ether. The residue was recovered and dried under vacuum at 40 °C (198 mg; 59 %).

*2.2.10. Synthesis of hybrid material **3b'***

Hybrid material **3b'** was prepared through the deprotonation of hybrid **3b**. Solid **3b** was washed with a saturated solution of sodium bicarbonate (3x40 mL), methanol (2x40 mL), and with diethyl ether (1x40 mL). The obtained black solid was dried under vacuum (100 mg).

*2.2.11. Synthesis of hybrid material **3c***

In a 5 mL glass vial, imidazolium salt **1c** (1 mmol, 404 mg) and dimethylurea (8 mmol, 720 mg) were added in 1:4 ratio with respect to bromide ions. The two solid components were allowed to mix at 80 °C for 2 h, under stirring (500 rpm). Once the DEM formed, MWCNTs (50 mg) were added and the mixture was heated at 80 °C for 30 min. AIBN (2.5 mol%, 9 mg) was added under Ar atmosphere and the reaction mixture was allowed to react at 80 °C for 40 min. The obtained dark residue was transferred into a centrifuge tube and methanol was added. The residue was subjected to centrifugation and the supernatant was removed. The solid was further washed with methanol, and diethyl ether. The washings were combined and dried under vacuum to recover the corresponding HBD. The residue was recovered and dried under vacuum at 40 °C (435 mg; 95 %).

*2.2.12. Synthesis of hybrid material **3d***

In a 5 mL glass vial, imidazolium salt **1d** (0.5 mmol, 203 mg) and dimethylurea (4 mmol, 360 mg) were added in 1:4 ratio with respect to bromide ions. The two solid components were allowed to mix at 80 °C for 2 h, under stirring (500 rpm). Once the DEM formed, MWCNTs (25 mg) were added and the mixture was heated at 80 °C for 30 min. AIBN (5 mol%, 9 mg) was added under Ar atmosphere and the reaction mixture was allowed to react at 80 °C for 40 min. The obtained dark residue was transferred into a centrifuge tube by adding methanol. The residue was subjected to centrifugation and the supernatant was removed. The solid was further washed with methanol, and diethyl ether. The washings were combined and dried under vacuum to recover the corresponding HBD. The residue was recovered and dried under vacuum at 40 °C (182 mg; 83 %).

*2.2.13. Synthesis of hybrid material **3e***

In a 5 mL glass vial, imidazolium salt **1e** (0.5 mmol, 225 mg) and dimethylurea (4 mmol, 360 mg) were added in 1:4 ratio with respect to bromide ions. The two solid components were allowed to mix at 80 °C for 2 h, under stirring (500 rpm). Once the DEM formed, MWCNTs (25 mg) were added and the mixture was heated at 80 °C for 30 min. AIBN (5 mol%, 9 mg) was added under Ar atmosphere and the reaction mixture was allowed to react at 80 °C for 40 min. The obtained dark residue was transferred into a centrifuge tube and methanol was added. The residue was subjected to centrifugation and the supernatant was removed. The solid was further washed with methanol, and diethyl ether. The washings were combined and dried under vacuum to recover the corresponding HBD. The residue was recovered and dried under vacuum at 40 °C (233 mg; 93 %).

2.2.14. Conventional polymerization of MWCNTs using solvent as dispersion medium

In a two-neck round-bottom flask, a suspension of MWCNTs (50 mg) and imidazolium salt **1c** (1 mmol, 404 mg) in absolute ethanol (5 ml) was sonicated for 20 min. Afterwards, AIBN (2.5 mol%, 9 mg) was added and argon was bubbled in the reaction mixture for 20 min. The mixture was then heated at 80 °C. After 20 h the solid was washed with methanol and diethyl ether and recovered by centrifugation. The residue was recovered and dried under vacuum at 40 °C (425 mg; 94 %).

*2.2.15. Synthesis of **Poly 1a***

In a 5 mL glass vial, imidazolium salt **1a** (1.5 mmol, 328.5 mg) and urea (6 mmol, 360.0 mg) were added in 1:4 ratio with respect to bromide ions. The two solid components were allowed to mix at 80 °C for 2 h, under stirring (500 rpm). AIBN (5 mol%, 12 mg) was added under Ar atmosphere and the reaction mixture was allowed to react at 80 °C for 40 min. The obtained white residue was transferred into a centrifuge tube and methanol was added. The residue was subjected to centrifugation and the supernatant was removed. The solid was further washed with methanol, and diethyl ether. The residue was recovered and dried under vacuum at 40 °C (304 mg; 92 %). For ^{13}C-CPMAS-TOSS NMR see Fig. S15.

2.2.16. Catalytic experiments

Catalytic experiments were carried out in a Cambridge Design Bullfrog batch reactor with temperature control and mechanical stirring. Before each experiment, the material was dried overnight in a vacuum oven at 60 °C. In each test, the catalyst was added to 24 mL of epichlorohydrin in a Teflon vial, under solvent-free conditions. After closing the reactor, the mixture was stirred at 500 rpm. The system was then purged for 10 min with N_2 before the addition of 25 bar of CO_2. After this, the system was heated at 150 °C with a rate of 5 °C/min. The reaction mixture was stirred at 150 °C for 3 h. The reactor was cooled down to room temperature and then it was depressurized. The separation of the catalyst from the reaction mixture was easily performed by centrifugation (15 min at 4500 rpm). The supernatant was analyzed by ^{1}H NMR.

2.2.17. Recycling test

The recyclability tests were carried out in the reaction between epichlorohydrin and CO_2. At the end of the reaction, the material **3a** was recovered by centrifugation and washed several times with toluene, ethanol and once with diethyl ether. Before every centrifugation, the catalyst was sonicated in the washing solvent up to get a good dispersion. After drying at 60 °C under vacuum, the catalyst was reused in the same reaction maintaining the ratio between moles of catalyst and moles of epoxides.

3. Results and discussion

The preparation of novel DEM systems containing polymerizable HBA species, namely mono- and bis-vinyl imidazolium salts, was conducted by selecting urea and dimethylurea (DMU) as hydrogen bond donors. Two different HBA/HBD ratios of 1:2 and 1:4 with respect to bromide ions were chosen. In the proposed methodology, the pivotal component of the eutectic mixture is the hydrogen bond acceptor, as it is the active agent directly involved in the polymerization reaction. In order to achieve structural variability of the final hybrid material, different mono- and bis-vinyl imidazolium bromide monomers **1a-e**, endowed with hydroxyl or amine groups, included in the spacer or side chain, were synthetized (*vide infra* Scheme 1). The eutectic mixtures were generated after two hours at 80 °C from the two solid components (Fig. S1).

Differential Scanning Calorimetry (DSC) was performed to investigate the thermal behaviour of the prepared DEM systems (Fig. 1a–b). Each sample was analyzed with a heating and cooling temperature ramp of 10 °C min^{-1}. DSC analysis confirms the successful formation of the DEM systems (solid lines) since their melting temperatures were lower than both the parent imidazolium salts (dashed lines **1a-e**) and the hydrogen bond donors (urea and DMU, red lines). Except for DEM **2a**, which is liquid at room temperature and shows no crystallization peak until −40 °C, and DEM **2b** that displays only a melting peak, DEMs **2c-e** showed a reproducible behaviour for three cycles, with the presence of melting and crystallization peaks (not shown in Fig. 1). Moreover, bis-vinyl imidazolium salt **1e** (dashed yellow line) exhibits no melting peak in the range of temperature examined (up to 120 °C).

Once established that DEMs were formed, they were exploited as efficient and reactive dispersing media for carbon nanotubes. In such a way, a series of novel hybrid materials based on MWCNT/poly-imidazolium salts **3a-e** were prepared through a convenient and straightforward methodology. The radical polymerization initiated by

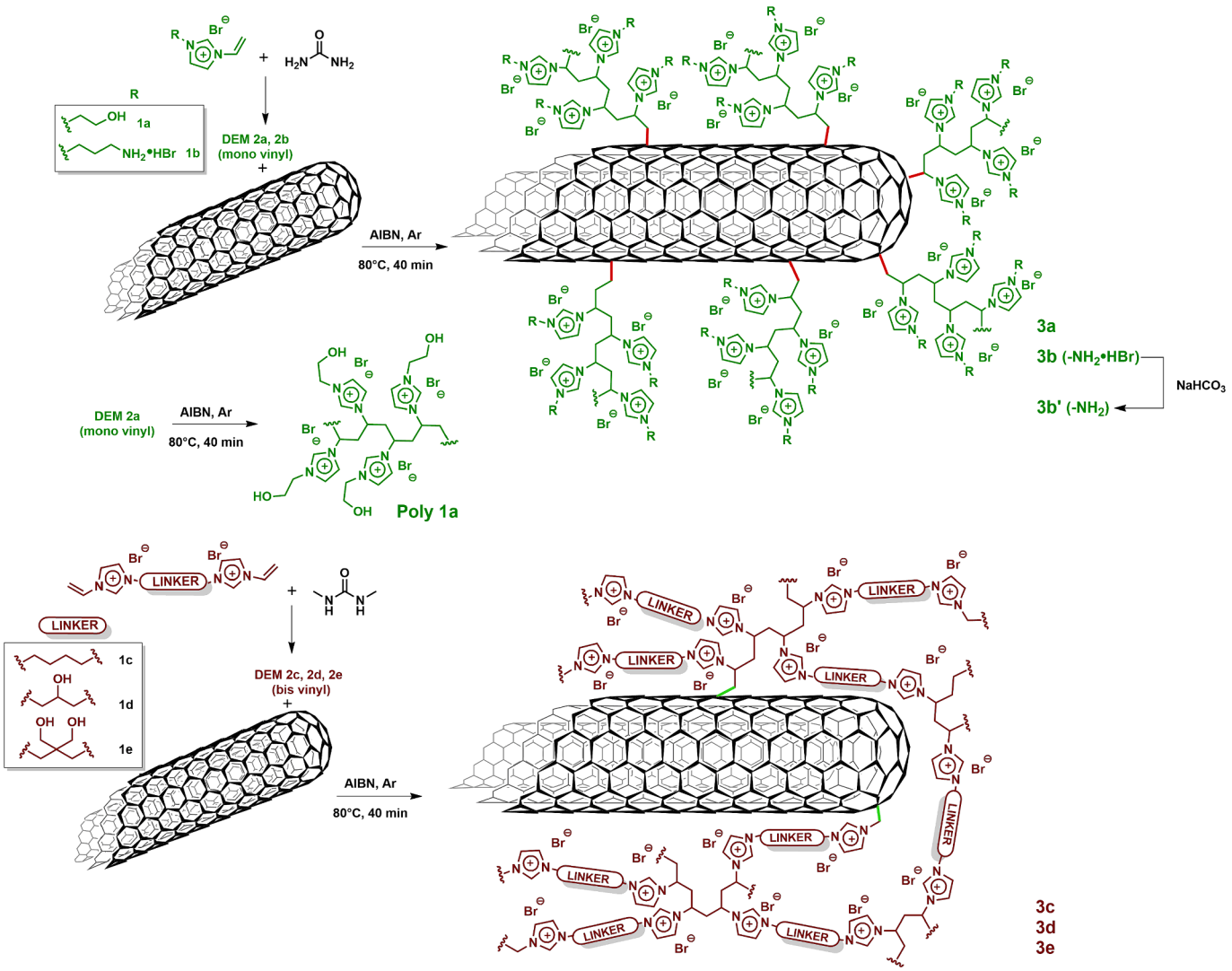

Scheme 1. Synthetic procedure for the preparation of materials **3a-e** and **Poly 1a.**

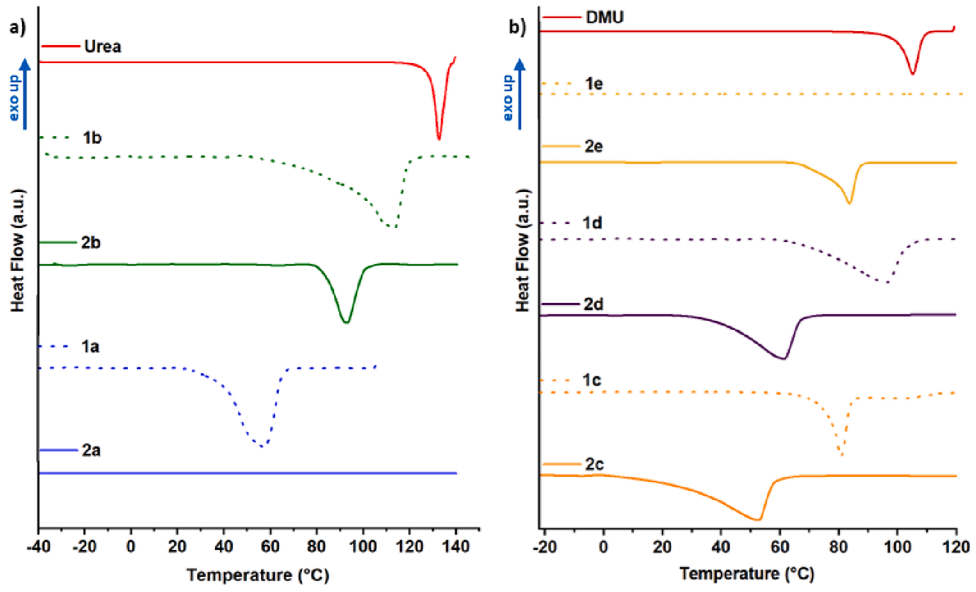

Fig. 1. Differential scanning calorimetry (DSC) thermograms of (a) vinyl imidazolium salts **1a-b**, DEM system **2a-b**, and urea; (b) vinyl imidazolium salts **1c-e**, DEM systems **2c-e**, and dimethylurea.

the thermal decomposition of 2,2′-azobis(isobutyronitrile) (AIBN) at 80 °C within the different DEM media **2a-e**, based on mono- or bis-vinyl imidazolium salts **1a-e**, in the presence of MWCNTs, resulted in highly functionalized hybrid materials in just 40 min (Scheme 1). Once AIBN is added, the reaction mixture quickly polymerizes by forming a solid mixture in which the DEM no longer exists. This strategy represents a versatile approach to get easy access to functionalized carbon nanotubes with different functional groups, which can be in turn post-modified. Thermogravimetric analysis under a nitrogen flow was employed to analyze the thermal profiles of the resulting hybrids MWCNT/polyimidazolium salts **3a-e** (Fig. 2a–b). All the materials proved to be very stable up to 270 °C, a temperature beyond which they start to decompose, except for material **3b'**, endowed of amino-groups in the side chains, which starts to degrade at a lower temperature of *ca.* 160 °C, and shows a marked decomposition process above 200 °C. The good thermal stability of the final hybrids is promising for their possible use under heating regimes. Thermogravimetric profile of pristine MWCNTs (*p*-MWCNTs, black line) showed very low weight loss (1 wt%) up to 700 °C. The functionalization loadings of materials **3a-e** were then estimated by evaluating their weight losses at 700 °C. The following values were obtained: **3a** 3.6, **3b** 2.3, **3b'** 2.9, **3c** 4.2, **3d** 3.6, and **3e** 3.1 mmol/g of imidazolium units. The estimation of specific surface areas (SSA) was carried out using the Brunauer–Emmett–Teller (BET) method [54,55]. The resulting SSA values were relatively low, falling within the range of less than 15 m^2/g (Table S1), in agreement with those previously obtained for analogous CNFs/polyimidazolium salts hybrids [23,24,56,57].

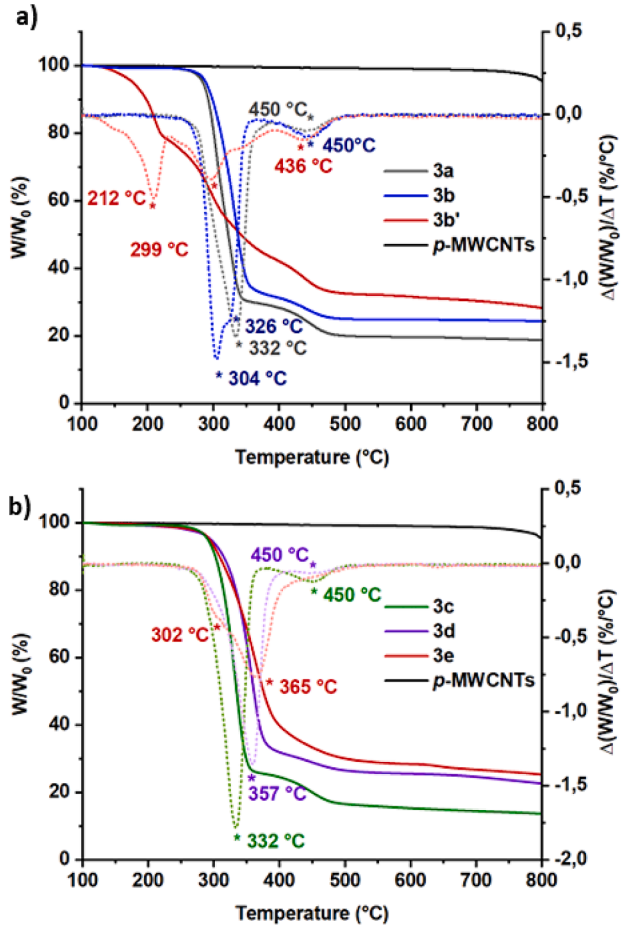

Fig. 2. TGA under N_2 flow and derivative thermogravimetric (DTG) curves (dotted lines) of a) *p*-MWCNT (black line), **3a** (grey line), **3b** (blue line) and **3b'** (red line), and b) *p*-MWCNT (black line), **3c** (green line), **3d** (violet line) and **3e** (red line). (For interpretation of the references to colour in this figure legend, the reader is referred to the web version of this article.)

Solid state ^{13}C-cross-polarization magic angle spinning - total suppression of sideband NMR (^{13}C-CPMAS-TOSS NMR) spectra of hybrid materials **3a-e** were collected and reported in Fig. 3. In the spectra, the signals of the aromatic carbon atoms of imidazolium moieties can be observed in the region between 115–150 ppm, while the signals associated with aliphatic carbon atoms are in the upfield region of the spectrum, ranging from 20 to 70 ppm. Additionally, the successful outcome of the polymerization process was confirmed by the absence of any signals in the 100–115 ppm region, where carbon atoms of the vinyl group typically resonate.

The evidence of the good outcome of the polymerization process was also confirmed by Fourier-transform infrared (FT-IR) spectroscopy, comparing the spectra of the imidazolium salts precursors with the spectra of the corresponding final hybrid materials (Fig. S2). FT-IR spectra of monomers **1a-e** (Fig. S2, red lines) show the typical bands associated with the C = C stretching of vinyl group of the imidazolium functionalities centred at 1620–1690 cm^{-1} and two bands at 920–960 cm^{-1} corresponding to the C–H bending.

As expected, these peaks disappear in the spectra of the hybrid materials **3a-e** (black lines), confirming the successful polymerization. Furthermore, the highly hygroscopic nature of the polymerized imidazolium salt results in the presence of a wide absorption peak between 3200–3500 cm^{-1}, attributable to the stretching of O–H bonds, and a moderate absorption at 1550 cm^{-1} arising from the bending of H–O–H bonds of the adsorbed water.

All the prepared hybrid materials were subjected to Raman spectroscopic analysis (Fig. S3), which made it possible to assess the covalent functionalization of carbon nanotubes through the change in the intensity ratio of the D band to the G band (I_D/I_G) compared to I_{D0}/I_{G0} ratio in the pristine CNTs. In particular, in the material **3a**, an increased normalized I_D/I_G ratio from the I_{D0}/I_{G0} ratio of 1.16 was found, proving the attachment onto the CNTs surface. Raman spectra of materials **3b**, **3b'**, and **3c** revealed no remarkable differences from Raman spectrum of *p*-MWCNTs. In order to interpret these results, it is necessary to take into account both the nature of the support material, being MWCNTs, and the functionalization process involved, namely radical polymerization. Indeed, despite the high degree of functionalization of the obtained materials, minimal disruption of the π-system of the outermost nanotube layer and thus minimal changes in the corresponding Raman spectra are obtained. Unfortunately, materials **3d** and **3e** gave rise to intense fluorescence emissions, upon excitation with all the laser wavelengths used (532, 633, and 785 nm), which hindered the acquisition of the Raman spectra.

Transmission electron microscopy (TEM) was used to investigate the

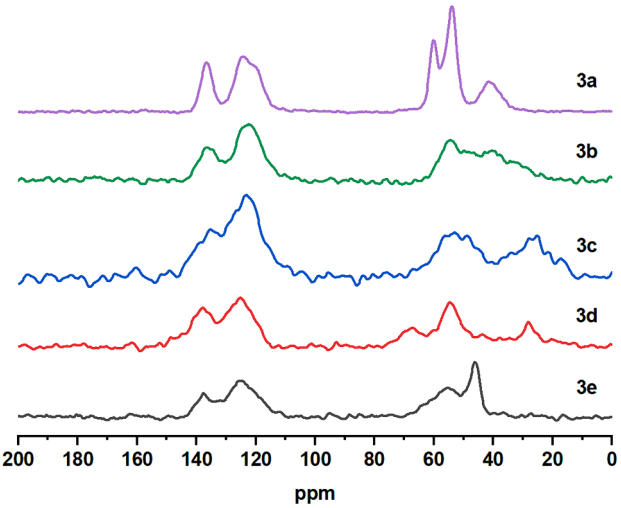

Fig. 3. ^{13}C-CPMAS-TOSS NMR solid state of hybrid materials **3a-e**.

morphology of the prepared hybrid materials. The micrographs of these hybrids (Fig. 4b–g) were compared with those of *p*-MWCNTs (Fig. 4a). Despite the random nature of the polymerization process, CNTs exert a templating effect on the polymeric network, which grows around the carbonaceous skeleton, as already observed by us, in the case of bis-vinyl imidazolium salts, when CNTs were used as support materials [22,23,26,27,56,57]. It is worth to note that in all cases, regardless of the nature of the monomer (mono- or bis-vinyl imidazolium salt), the polymerization led to the formation of an unusually compact MWCNTs-coating. As said above, the immobilization of the polymerizable HBA component of the DEM system onto the CNTs surface causes the modification of the HBD/HBA molar ratio resulting in a eutectic rupture and phase segregation by means of a spinodal-like decomposition induced by the polymerization process and the formation of a polymer-depleted solid phase, mainly consisting of the inert HBD component of the DEM [40,43,44]. This phenomenon could play a role on the morphology of the obtained materials, since DEM system could act as additional structure directing agent on the growth of the polymeric matrix.

The polymerization in DEM media formed from mono-vinyl monomers as HBA species led to the formation of well-dispersed and individualized nano-objects having mean diameters larger than that of *p*-MWCNTs (Fig. 4b–d). The size distribution histograms of *p*-MWCNTs and materials **3a**, **3b**, and **3b'**, shown in Fig. 4h, highlight this increase in average size since *p*-MWCNTs have a mean diameter of 14 ± 7 nm (n = 150 counts), whereas materials **3a**, **3b**, and **3b'** show bigger diameters of 33 ± 8 (n = 155 counts), 35 ± 8 (n = 160 counts), and 42 ± 10 (n = 55 counts), respectively. Once again, the use of bis-vinyl monomers as polymerizable HBA species resulted in the covering of CNTs skeleton, although the possibility of cross-linking led to the formation of numerous aggregates that significantly lowered the number of individualized nano-objects hampering and making statistically not significant the construction of a size distribution curve. However, no objects with a diameter bigger than 50 nm have been identified. Regarding this last observation, it is noteworthy to compare material **3c** (4.2 mmol/g) obtained by DEM-mediated functionalization with the same material previously obtained by us with the conventional method dissolving the bis-vinyl imidazolium salt **1c** in ethanol (4.5 mmol/g).[23] Despite the two synthetic strategies gave rise to materials with similar functionalization degrees, significant differences in means diameters were obtained. Specifically, the conventional methodology resulted in a thicker polymeric coating of *ca.* 150 nm against a more compact layer of 50 nm in the case of DEM-mediated functionalization (Fig. 5). This outcome

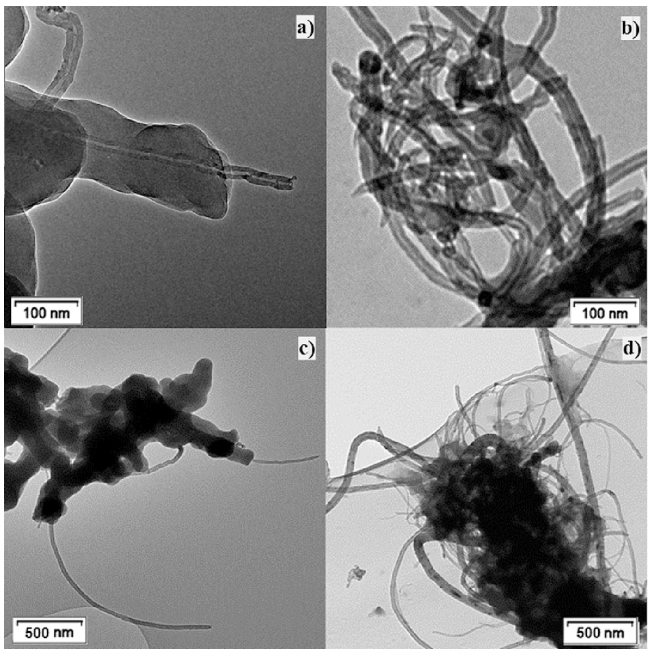

Fig. 5. Transmission electron microscopy images of: (a and c) hybrid material obtained in diluted solvent conditions (2.6 mg/mL of MWCNTs in ethanol)[23] and (b and d) hybrid material **3c**.

can be explained by considering the different nature of the two reaction media, namely ethanol and the DEM system, in which polymerization takes place. Indeed, the concentration of the monomer **1c** is lower in ethanol with respect to that in DEM system **2c** (**1c**/DMU). Therefore, when ethanol was used as solvent, the low monomer concentration could cause a lower number of anchored vinyl moieties on the surface of MWCNT which, consequently, polymerize in a less compact manner giving a material with a large radius around the MWCNT; conversely the higher monomer concentration in the DEM **2c**, along with the eutectic rupture and phase segregation, could result in a greater number of anchored vinyl moieties that leads to a higher compact structure with a much lower radius (*ca.* 50 nm). In the light of the above, in addition to act as a dispersing medium for CNTs and reactant for the CNTs-templated polymerization process, DEM plays a third role since it can

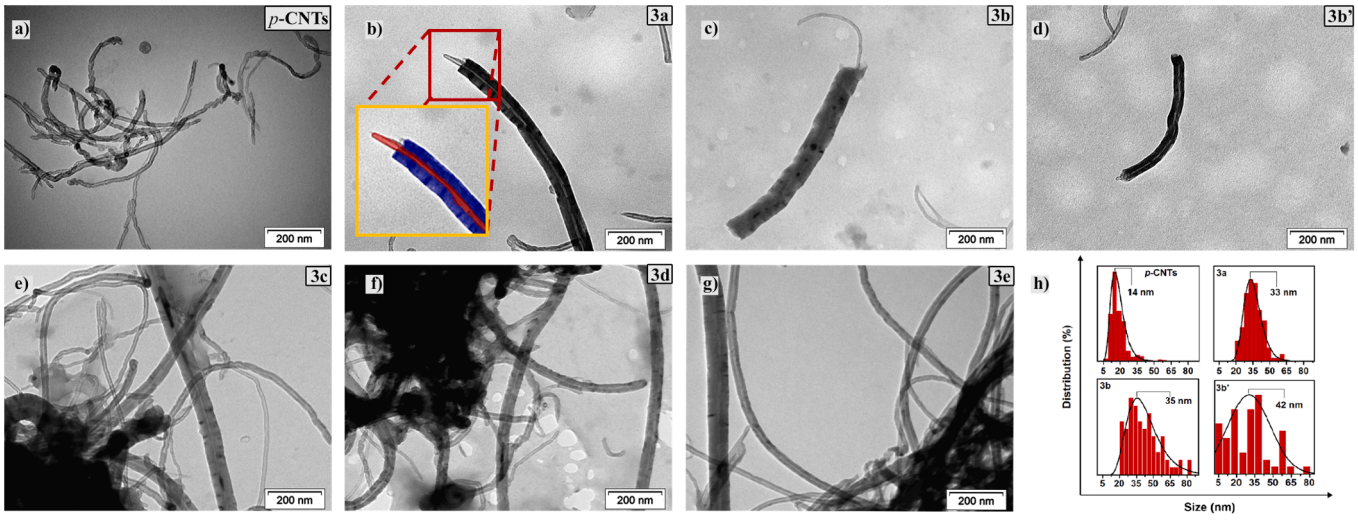

Fig. 4. Transmission electron microscopy images of: (a) *p*-MWCNTs; (b) **3a**, in the inset the polymer coating is marked in blue and the nanotube in red; (c) **3b**; (d) **3b'**; (e) **3c**;(f) **3d**; (g) **3e** and (h) size distribution histograms of *p*-MWCNTs, **3a**, **3b** and **3b'**. (For interpretation of the references to colour in this figure legend, the reader is referred to the web version of this article.)

actively affect the morphology of the obtained material.

The sustainability of the whole can be further increased through the possible recovery and reuse of the inert HBD component at the end of the reaction. When mixed with fresh **1c**, recovered DMU reformed the corresponding DEM system.

Furthermore, when we carried out the conventional polymerization of the bis-vinyl imidazolium salt **1c,** a dispersion of 2.6 mg mL^{-1} of MWCNTs in ethanol was used [23]. In this case, a homogeneous material with a good degree of functionalization was obtained. Herein, we have been interested in investigating whether it was possible to reduce the amount of organic solvent using a concentration of 10 mg mL^{-1} of MWCNTs, namely the higher achievable suitable to ensure both a good dispersion of the nanotubes and the solubilization of the bis-vinyl imidazolium salt **1c**. Such conditions led to the obtainment of a physical mixture of CNTs supported and homopolymerized poly-imidazolium salt (Fig. 6) indicating that higher dilutions are needed to avoid the heterogeneity of the material.

This evidence further corroborates the green aspects of DEM-mediated functionalization of MWCNTs since it allows reducing the amounts of organic solvents used. Furthermore, regarding the functionalization with mono-vinyl salts, although a few examples have been reported, [58–61] when ethanol was used as dispersing medium, no polymerization was initiated under all the conditions tested by us. This emphasizes another advantage of DEM-mediated polymerization, which enables the preparation of new materials that would otherwise not be accessible.

Once characterized, all the hybrid materials **3a-e** were applied as heterogeneous catalysts in the reaction between CO_2 and epichlorohydrin into the corresponding cyclic carbonate. The catalytic performance of the hybrids was evaluated in terms of conversion, turnover number (TON, defined as moles of epoxide converted/moles of supported imidazolium bromide), turnover frequency (TOF = TON/time (h)) and recyclability. In order to study the effect of the different linear and cross-linked polymer supported onto MWCNTs, six catalytic tests were carried out in the reaction between carbon dioxide and epichlorohydrin under solvent-free conditions, at 150 °C, and without using any co-catalytic species (Table 1**, entries 1**–**6**).

From this preliminary investigation, **3a** resulted the more active material. This behaviour can be ascribed to the different structures of the hybrids. The better catalytic activity of **3a** could be explained by the linear morphology of the polymer supported on the MWCNTs, leading to a higher accessibility of the imidazolium units to the substrates. To corroborate this hypothesis, we performed two additional catalytic

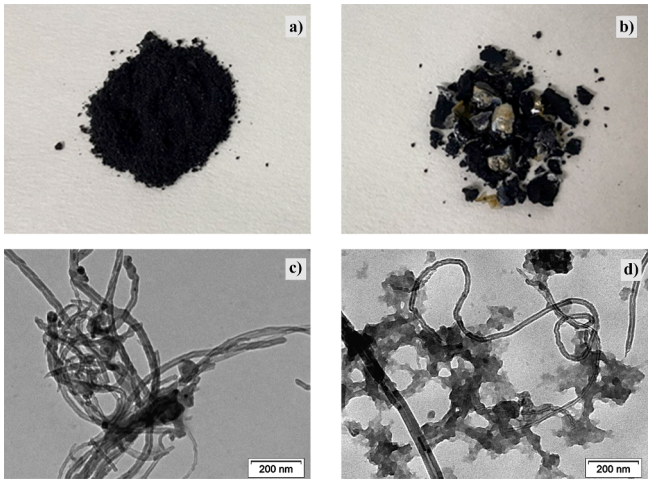

Fig. 6. Appearance of (a) hybrid material **3c** and (b) the same hybrid material prepared using a concentration of 10 mg/mL of MWCNTs in ethanol. Transmission electron microscopy images of: (c) material **3c** and (d) material obtained in concentrated solvent conditions (10 mg/mL of MWCNTs in ethanol).

Table 1
Conversion of epichlorohydrin and CO_2 into the cyclic carbonate.[a]

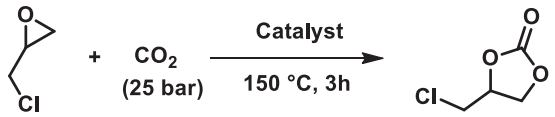

Entry	Catalyst	Conversion(%)[b]	TON[c]	TOF[c]
1	**3a**	70	1020	340
2	**3b**	56	640	210
3	**3b'**	57	970	320
4	**3c**	70	850	280
5	**3d**	47	650	210
6	**3e**	25	430	145
7	**Poly 1a**	45	660	220
8	**p-MWCNTs**	traces	–	–

[a] Reaction conditions: epichlorohydrin (306 mmol), catalyst 60 mg (**3a** 0.21 mmol Br^-; **3b** 0.27 mmol Br^-; **3b'** 0.18 mmol Br^-; **3c** 0.25 mmol Br^-; **3d** 0.22 mmol Br^-; **3e** 0.18 mmol Br^-), 25 bar CO_2, 150 °C, 3 h, 500 rpm.
[b] Determined by ^1H NMR (Fig. S16–23).
[c] TON and TOF values calculated based on the bromide content in the hybrid materials.

experiments with homopolymerized **1a** (**Poly 1a**, Scheme 1) and *p*-MWCNTs (Table 1**, entries 7**–**8**). The results showed that **Poly 1a** possesses a lower catalytic activity compared to the hybrid supported **3a**, whereas *p*-MWCNTs allowed to obtain only traces of the product. Moreover, the TON and TOF values (1020 and 340 h^{-1}) of hybrid **3a** are almost twice as high as the values of **Poly 1a** (660 and 220 h^{-1}). These findings underline the importance of combining polymer with MWCNTs, as an inert support, to produce hybrid materials that show a significant improvement in catalytic performance.

The hybrid material **3a** was chosen for further investigation. Again, the reaction between CO_2 and epichlorohydrin was selected as benchmark reaction to study the recyclability of the hybrid material. Three consecutive cycles were performed without significant loss in catalytic activity (Fig. S4). After each cycle, the material was recovered through centrifugations. Subsequently, it was washed with toluene, ethanol, and diethyl ether, requiring no further activation treatments. Once recovered, the recycled hybrid material **3a** was characterized by means of TEM (Fig. S24) and showed only minor differences with respect to the fresh material. In particular, the average diameter of the used and that of the fresh catalyst resulted in good agreement, namely 31 ± 12 nm (n = 96 counts) vs 33 ± 8 nm, respectively.

Finally, the catalytic activity of material **3a** was compared with others reported heterogeneous catalytic systems containing Lewis base species (Table S2). In general, **3a** proved to have a better performance with respect to the catalysts taken into account for the conversion of CO_2 into cyclic carbonates.

4. Conclusion

In conclusion, we reported a novel synthetic strategy based on the triple role of DEMs able to act as convenient dispersion media for MWCNTs, efficient reactive systems, and also as structure-directing agents for the polymerization process. This methodology was exploited for the functionalization of MWCNTs by means of the radical polymerization of mono- or bis-vinyl imidazolium salts endowed with different functional groups (–OH, $–NH_2$, $–NH_3^+Br^-$) used as HBA species of the eutectic mixtures. The new hybrid materials were fully characterized by means of TGA, ^{13}C-CPMAS TOSS NMR, FT-IR, SSA, Raman, and TEM analyses. This latter technique revealed the effective coverage of the CNTs structure by the polymeric matrix. Whereas CNTs acted as template for the growth of the polymeric network, the DEM systems played a complementary role on the morphology of the hybrid materials, which were characterized by the presence of a compact polymeric

matrix around the CNTs structure. The hybrids were successfully applied as heterogeneous catalysts for the conversion of carbon dioxide and epichlorohydrin into the corresponding cyclic carbonate and the best performing material was further investigated to carry out recycling studies for three consecutive runs. Interestingly, the best hybrid material displayed a catalytic activity almost double in terms of TON and TOF with respect to the corresponding unsupported poly ionic liquid. This promising and eco-friendly strategy paves the way for the obtainment of different functional materials in which both the identity of DEM and that of support material, namely carbon nanoform or properly functionalized metal oxide (SiO_2, TiO_2, Al_2O_3, etc.), can be varied. In addition, the use of these hybrids both for the immobilization of metal nanoparticles and for the generation of N-doped carbon nanotubes is currently underway.

CRediT authorship contribution statement

Laura Valentino: Writing – review & editing, Writing – original draft, Visualization, Validation, Methodology, Investigation, Data curation. **Riccardo Di Forti:** Investigation. **Anthony Morena:** Investigation. **Carmela Aprile:** Writing – review & editing, Supervision, Funding acquisition. **Michelangelo Gruttadauria:** Writing – review & editing, Supervision, Conceptualization. **Francesco Giacalone:** Writing – review & editing, Supervision, Funding acquisition, Conceptualization. **Vincenzo Campisciano:** Writing – review & editing, Visualization, Validation, Methodology, Data curation, Conceptualization.

Declaration of competing interest

The authors declare that they have no known competing financial interests or personal relationships that could have appeared to influence the work reported in this paper.

Data availability

Data will be made available on request.

Acknowledgements

This research was funded by University of Palermo and the Italian Ministry of Education (PRIN 2017 project no. 2017W8KNZW). We also thank MUR for funding, SiciliAn MicronanOTecH Research And Innovation CEnter "SAMOTHRACE" (MUR, PNRR-M4C2, ECS_00000022), spoke 3 - University of Palermo "S2-COMMs - Micro and Nanotechnologies for Smart & Sustainable Communities". The authors acknowledge Dr. Luca Fusaro and Mr. Oliver Garot for their support to the NMR experiments. This research used resources of PC2 (Plateforme Technologique Physico-Chemical Characterization) and MORPH-IM (Morphology & Imaging) technology platforms located at the University of Namur. We acknowledge Dr. Carla Rizzo from the University of Palermo for her support on DSC analysis and Prof. S. Agnello (ATeN Center, University of Palermo) for the access to Raman spectroscopy.

Appendix A. Supplementary data

Supplementary data to this article can be found online at https://doi.org/10.1016/j.cej.2024.151447.

References

[1] D.S. Su, S. Perathoner, G. Centi, Nanocarbons for the Development of Advanced Catalysts, Chem. Rev. 113 (2013) 5782–5816, https://doi.org/10.1021/cr300367d.
[2] J.H. Lehman, M. Terrones, E. Mansfield, K.E. Hurst, V. Meunier, Evaluating the characteristics of multiwall carbon nanotubes, Carbon 49 (2011) 2581–2602, https://doi.org/10.1016/j.carbon.2011.03.028.
[3] V. Campisciano, M. Gruttadauria, F. Giacalone, Modified Nanocarbons for Catalysis, ChemCatChem 11 (2019) 90–133, https://doi.org/10.1002/cctc.201801414.
[4] Rümmeli, M. H.; Ayala, P.; Pichler, T., Carbon Nanotubes and Related Structures: Production and Formation. In *Carbon Nanotubes and Related Structures*, Dirk M. Guldi; Martín, N., Eds. Wiley-VCH Weinheim, Germany, **2010**; pp 1-21.
[5] D. Jariwala, V.K. Sangwan, L.J. Lauhon, T.J. Marks, M.C. Hersam, Carbon nanomaterials for electronics, optoelectronics, photovoltaics, and sensing, Chem. Soc. Rev. 42 (2013) 2824–2860, https://doi.org/10.1039/C2CS35335K.
[6] M. Melchionna, S. Marchesan, M. Prato, P. Fornasiero, Carbon nanotubes and catalysis: the many facets of a successful marriage, Catal. Sci. Technol. 5 (2015) 3859–3875, https://doi.org/10.1039/C5CY00651A.
[7] Y. Yang, X. Yang, Y. Yang, Q. Yuan, Aptamer-functionalized carbon nanomaterials electrochemical sensors for detecting cancer relevant biomolecules, Carbon 129 (2018) 380–395, https://doi.org/10.1016/j.carbon.2017.12.013.
[8] Z. Yang, J. Ren, Z. Zhang, X. Chen, G. Guan, L. Qiu, Y. Zhang, H. Peng, Recent Advancement of Nanostructured Carbon for Energy Applications, Chem. Rev. 115 (2015) 5159–5223, https://doi.org/10.1021/cr5006217.
[9] S. Kumar, H.K. Sidhu, A.K. Paul, N. Bhardwaj, N.S. Thakur, A. Deep, Bioengineered multi-walled carbon nanotube (MWCNT) based biosensors and applications thereof, Sens. Diagn. 2 (2023) 1390–1413, https://doi.org/10.1039/D3SD00176H.
[10] A. Bianco, K. Kostarelos, C.D. Partidos, M. Prato, Biomedical applications of functionalised carbon nanotubes, Chem. Commun. (2005) 571–577, https://doi.org/10.1039/B410943K.
[11] A. Bianco, K. Kostarelos, M. Prato, Applications of carbon nanotubes in drug delivery, Curr. Opin. Chem. Bio. 9 (2005) 674–679, https://doi.org/10.1016/j.cbpa.2005.10.005.
[12] M. Barrejón, S. Marchesan, N. Alegret, M. Prato, Carbon nanotubes for cardiac tissue regeneration: State of the art and perspectives, Carbon 184 (2021) 641–650, https://doi.org/10.1016/j.carbon.2021.08.059.
[13] A. Hirsch, Functionalization of Single-Walled Carbon Nanotubes, Angew. Chem. Int. Ed. 41 (2002) 1853–1859, https://doi.org/10.1002/1521-3773(20020603)41:11<1853::AID-ANIE1853>3.0.CO;2-N.
[14] D. Tasis, N. Tagmatarchis, A. Bianco, M. Prato, Chemistry of Carbon Nanotubes, Chem. Rev. 106 (2006) 1105–1136, https://doi.org/10.1021/cr050569o.
[15] P. Singh, S. Campidelli, S. Giordani, D. Bonifazi, A. Bianco, M. Prato, Organic functionalisation and characterisation of single-walled carbon nanotubes, Chem. Soc. Rev. 38 (2009) 2214–2230, https://doi.org/10.1039/B518111A.
[16] K.J. Ziegler, Z. Gu, H. Peng, E.L. Flor, R.H. Hauge, R.E. Smalley, Controlled Oxidative Cutting of Single-Walled Carbon Nanotubes, J. Am. Chem. Soc. 127 (2005) 1541–1547, https://doi.org/10.1021/ja044537e.
[17] T. Fukushima, A. Kosaka, Y. Ishimura, T. Yamamoto, T. Takigawa, N. Ishii, T. Aida, Molecular Ordering of Organic Molten Salts Triggered by Single-Walled Carbon Nanotubes, Science 300 (2003) 2072–2074, https://doi.org/10.1126/science.1082289.
[18] T. Fukushima, T. Aida, Ionic Liquids for Soft Functional Materials with Carbon Nanotubes, Chem. Eur. J. 13 (2007) 5048–5058, https://doi.org/10.1002/chem.200700554.
[19] J. Wang, H. Chu, Y. Li, Why Single-Walled Carbon Nanotubes Can Be Dispersed in Imidazolium-Based Ionic Liquids, ACS Nano 2 (2008) 2540–2546, https://doi.org/10.1021/nn800510g.
[20] M. Tunckol, J. Durand, P. Serp, Carbon nanomaterial–ionic liquid hybrids, Carbon 50 (2012) 4303–4334, https://doi.org/10.1016/j.carbon.2012.05.017.
[21] M.L. Polo-Luque, B.M. Simonet, M. Valcárcel, Functionalization and dispersion of carbon nanotubes in ionic liquids, Trends Anal. Chem. 47 (2013) 99–110, https://doi.org/10.1016/j.trac.2013.03.007.
[22] A. Morena, V. Campisciano, A. Comès, L.F. Liotta, M. Gruttadauria, C. Aprile, F. Giacalone, A Study on the Stability of Carbon Nanoforms-Polyimidazolium Network Hybrids in the Conversion of CO2 into Cyclic Carbonates: Increase in Catalytic Activity after Reuse, Nanomaterials 11 (2021) 2243, https://doi.org/10.3390/nano11092243.
[23] V. Campisciano, C. Calabrese, L.F. Liotta, V. La Parola, A. Spinella, C. Aprile, M. Gruttadauria, F. Giacalone, Templating effect of carbon nanoforms on highly cross-linked imidazolium network: Catalytic activity of the resulting hybrids with Pd nanoparticles, Appl. Organomet. Chem. 33 (2019) e4848, https://doi.org/10.1002/aoc.4848.
[24] C. Calabrese, L.F. Liotta, E. Carbonell, F. Giacalone, M. Gruttadauria, C. Aprile, Imidazolium-Functionalized Carbon Nanohorns for the Conversion of Carbon Dioxide: Unprecedented Increase of Catalytic Activity after Recycling, ChemSusChem 10 (2017) 1202–1209, https://doi.org/10.1002/cssc.201601427.
[25] M. Buaki-Sogó, A. Vivian, L.A. Bivona, H. García, M. Gruttadauria, C. Aprile, Imidazolium functionalized carbon nanotubes for the synthesis of cyclic carbonates: reducing the gap between homogeneous and heterogeneous catalysis, Catal. Sci. Technol. 6 (2016) 8418–8427, https://doi.org/10.1039/C6CY01068G.
[26] L. Valentino, V. Campisciano, C. Célis, V. Lemaur, R. Lazzaroni, M. Gruttadauria, C. Aprile, F. Giacalone, Highly cross-linked bifunctional magnesium porphyrin-imidazolium bromide polymer: Unveiling the key role of co-catalysts proximity for CO2 conversion into cyclic carbonates, J. Catal. 428 (2023) 115143, https://doi.org/10.1016/j.jcat.2023.115143.
[27] V. Campisciano, L. Valentino, A. Morena, A. Santiago-Portillo, N. Saladino, M. Gruttadauria, C. Aprile, F. Giacalone, Carbon nanotube supported aluminum porphyrin-imidazolium bromide crosslinked copolymer: A synergistic bifunctional catalyst for CO2 conversion, J. CO2 Util. 57 (2022) 101884, https://doi.org/10.1016/j.jcou.2022.101884.
[28] C.M.Q. Le, X.T. Cao, T.T.K. Tu, W.-K. Lee, K.T. Lim, Facile covalent functionalization of carbon nanotubes via Diels-Alder reaction in deep eutectic solvents, Appl. Surf. Sci. 450 (2018) 122–129, https://doi.org/10.1016/j.apsusc.2018.04.173.

[29] L. Chen, J. Deng, Y. Song, S. Hong, H. Lian, Highly Stable Dispersion of Carbon Nanotubes in Deep Eutectic Solvent for the Preparation of CNT-Embedded Carbon Xerogels for Supercapacitors, ChemElectroChem 6 (2019) 5750–5758, https://doi.org/10.1002/celc.201901611.
[30] A.T.S.C. Brandão, S. Rosoiu, R. Costa, A.F. Silva, L. Anicai, M. Enachescu, C. M. Pereira, Characterization of Carbon Nanomaterials Dispersions: Can Metal Decoration of MWCNTs Improve Their Physicochemical Properties? Nanomaterials 12 (2022) 99, https://doi.org/10.3390/nano12010099.
[31] J. Patiño, N. López-Salas, M.C. Gutiérrez, D. Carriazo, M.L. Ferrer, F. Monte, d., Phosphorus-doped carbon–carbon nanotube hierarchical monoliths as true three-dimensional electrodes in supercapacitor cells, J. Mater. Chem. A 4 (2016) 1251–1263, https://doi.org/10.1039/C5TA09210H.
[32] J. Płotka-Wasylka, M. de la Guardia, V. Andruch, M. Vilková, Deep eutectic solvents vs ionic liquids: Similarities and differences, Microchem. J. 159 (2020) 105539, https://doi.org/10.1016/j.microc.2020.105539.
[33] A.P. Abbott, D. Boothby, G. Capper, D.L. Davies, R.K. Rasheed, Deep Eutectic Solvents Formed between Choline Chloride and Carboxylic Acids: Versatile Alternatives to Ionic Liquids, J. Am. Chem. Soc. 126 (2004) 9142–9147, https://doi.org/10.1021/ja048266j.
[34] A.P. Abbott, G. Capper, D.L. Davies, R.K. Rasheed, V. Tambyrajah, Novel solvent properties of choline chloride/urea mixtures, Chem. Commun. (2003) 70–71, https://doi.org/10.1039/B210714G.
[35] E.L. Smith, A.P. Abbott, K.S. Ryder, Deep Eutectic Solvents (DESs) and Their Applications, Chem. Rev. 114 (2014) 11060–11082, https://doi.org/10.1021/cr300162p.
[36] M.C. Gutiérrez, F. Rubio, F. del Monte, Resorcinol-Formaldehyde Polycondensation in Deep Eutectic Solvents for the Preparation of Carbons and Carbon−Carbon Nanotube Composites, Chem. Mater. 22 (2010) 2711–2719, https://doi.org/10.1021/cm9023502.
[37] G. Carrasco-Huertas, R.J. Jiménez-Riobóo, M.C. Gutiérrez, M.L. Ferrer, F. del Monte, Carbon and carbon composites obtained using deep eutectic solvents and aqueous dilutions thereof, Chem. Commun. 56 (2020) 3592–3604, https://doi.org/10.1039/D0CC00681E.
[38] M.C. Gutiérrez, D. Carriazo, A. Tamayo, R. Jiménez, F. Picó, J.M. Rojo, M.L. Ferrer, F. del Monte, Deep-Eutectic-Solvent-Assisted Synthesis of Hierarchical Carbon Electrodes Exhibiting Capacitance Retention at High Current Densities, Chem. Eur. J. 17 (2011) 10533–10537, https://doi.org/10.1002/chem.201101679.
[39] J.D. Mota-Morales, M.C. Gutiérrez, M.L. Ferrer, R. Jiménez, P. Santiago, I. C. Sanchez, M. Terrones, F. Del Monte, G. Luna-Bárcenas, Synthesis of macroporous poly(acrylic acid)–carbon nanotube composites by frontal polymerization in deep-eutectic solvents, J. Mater. Chem. A 1 (2013) 3970–3976, https://doi.org/10.1039/C3TA01020A.
[40] F. del Monte, D. Carriazo, M.C. Serrano, M.C. Gutiérrez, M.L. Ferrer, Deep Eutectic Solvents in Polymerizations: A Greener Alternative to Conventional Syntheses, ChemSusChem 7 (2014) 999–1009, https://doi.org/10.1002/cssc.201300864.
[41] J.D. Mota-Morales, M.C. Gutiérrez, I.C. Sanchez, G. Luna-Bárcenas, F. del Monte, Frontal polymerizations carried out in deep-eutectic mixtures providing both the monomers and the polymerization medium, Chem. Commun. 47 (2011) 5328–5330, https://doi.org/10.1039/C1CC10391A.
[42] J.D. Mota-Morales, M.C. Gutiérrez, M.L. Ferrer, I.C. Sanchez, E.A. Elizalde-Peña, J. A. Pojman, F.D. Monte, G. Luna-Bárcenas, Deep eutectic solvents as both active fillers and monomers for frontal polymerization, J. Polym. Sci. 51 (2013) 1767–1773, https://doi.org/10.1002/pola.26555.
[43] J.P. Paraknowitsch, A. Thomas, Functional Carbon Materials From Ionic Liquid Precursors, Macromol. Chem. Phy. 213 (2012) 1132–1145, https://doi.org/10.1002/macp.201100573.
[44] M.C. Gutiérrez, D. Carriazo, C.O. Ania, J.B. Parra, M.L. Ferrer, F. del Monte, Deep eutectic solvents as both precursors and structure directing agents in the synthesis of nitrogen doped hierarchical carbons highly suitable for CO2 capture, Energy Environ. Sci. 4 (2011) 3535–3544, https://doi.org/10.1039/C1EE01463C.
[45] X. Yang, Y. Zhang, F. Liu, P. Chen, T. Zhao, Y. Wu, Deep eutectic solvents consisting of EmimCl and amides: Highly efficient SO2 absorption and conversion, Sep. Purif. Technol. 250 (2020) 117273, https://doi.org/10.1016/j.seppur.2020.117273.
[46] Z. Ren, X. Wu, H. Yu, F. Zhang, S. Tian, Z. Zhou, Effective separation of toluene from n-heptane with imidazolium-based deep eutectic solvents, Fuel 326 (2022) 124992, https://doi.org/10.1016/j.fuel.2022.124992.
[47] Y. Liu, Z. Cao, Z. Zhou, A. Zhou, Imidazolium-based deep eutectic solvents as multifunctional catalysts for multisite synergistic activation of epoxides and ambient synthesis of cyclic carbonates, J. CO2 Util. 53 (2021) 101717, https://doi.org/10.1016/j.jcou.2021.101717.
[48] W. Huang, H. Wang, W. Hu, D. Yang, S. Yu, F. Liu, X. Song, Degradation of polycarbonate to produce bisphenol A catalyzed by imidazolium-based DESs under metal-and solvent-free conditions, RSC Adv. 11 (2021) 1595–1604, https://doi.org/10.1039/D0RA09215K.
[49] T. Chen, Y. Xu, The Effect of DBU on Microstructure and CO2 Absorption of EmimCl-TEG and BmimCl-TEG Deep Eutectic Solvents, ChemistrySelect 8 (2023) e202301413.
[50] B. Kabane, G.G. Redhi, Thermodynamic properties and activity coefficients at infinite dilution for different solutes in deep eutectic solvent: 1-butyl-3-methylimidazolium chloride + glycerol, J. Mol. Liq. 311 (2020) 113216, https://doi.org/10.1016/j.molliq.2020.113216.
[51] S. Choudhury, U. Mahanta, R. Prasanna Venkatesh, T. Banerjee, Ionic liquid derived novel deep eutectic solvents as low viscous electrolytes for energy storage, J. Mol. Liq. 366 (2022) 120245, https://doi.org/10.1016/j.molliq.2022.120245.
[52] N. Li, R. Qu, X. Han, W. Lin, H. Zhang, Z.J. Zhang, The Counterion Effect of Imidazolium-Type Poly(ionic liquid) Brushes on Carbon Dioxide Adsorption, ChemPlusChem 84 (2019) 281–288, https://doi.org/10.1002/cplu.201800636.
[53] Y. Tan, M. Li, X. Ye, Z. Wang, Y. Wang, C. Li, Ionic liquid auxiliary exfoliation of WS2 nanosheets and the enhanced effect of hollow gold nanospheres on their photoelectrochemical sensing towards human epididymis protein 4, Sens. Actuators B Chem. 262 (2018) 982–990, https://doi.org/10.1016/j.snb.2018.02.066.
[54] M. Thommes, K. Kaneko, A.V. Neimark, J.P. Olivier, F. Rodriguez-Reinoso, J. Rouquerol, K.S.W. Sing, Physisorption of gases, with special reference to the evaluation of surface area and pore size distribution (IUPAC Technical Report), Pure Appl. Chem. 87 (2015) 1051–1069, https://doi.org/10.1515/pac-2014-1117.
[55] S. Brunauer, P.H. Emmett, E. Teller, Adsorption of Gases in Multimolecular Layers, J. Am. Chem. Soc. 60 (1938) 309–319, https://doi.org/10.1021/ja01269a023.
[56] I. Ziccarelli, R. Mancuso, F. Giacalone, C. Calabrese, V. La Parola, A. De Salvo, N. Della Ca, M. Gruttadauria, B. Gabriele, Heterogenizing palladium tetraiodide catalyst for carbonylation reactions, J. Catal. 413 (2022) 1098–1110, https://doi.org/10.1016/j.jcat.2022.08.007.
[57] V. Campisciano, R. Burger, C. Calabrese, L.F. Liotta, P. Lo Meo, M. Gruttadauria, F. Giacalone, Straightforward preparation of highly loaded MWCNT–polyamine hybrids and their application in catalysis, Nanoscale Adv. 2 (2020) 4199–4211, https://doi.org/10.1039/D0NA00291G.
[58] Y. Wang, Z. Ma, P. Liu, W. He, Flexible conductive energetic film based on energetic ionic liquids and carbon nanotubes for information security transient electronics, Chem. Eng. J. 473 (2023) 144981, https://doi.org/10.1016/j.cej.2023.144981.
[59] Y. Ding, A. Klyushin, X. Huang, T. Jones, D. Teschner, F. Girgsdies, T. Rodenas, R. Schlögl, S. Heumann, Cobalt-Bridged Ionic Liquid Polymer on a Carbon Nanotube for Enhanced Oxygen Evolution Reaction Activity, Angew. Chem. Int. Ed. 57 (2018) 3514–3518, https://doi.org/10.1002/anie.201711688.
[60] X. Feng, W. Gao, S. Zhou, H. Shi, H. Huang, W. Song, Discrimination and simultaneous determination of hydroquinone and catechol by tunable polymerization of imidazolium-based ionic liquid on multi-walled carbon nanotube surfaces, Anal. Chim. Acta 805 (2013) 36–44, https://doi.org/10.1016/j.aca.2013.10.044.
[61] B. Wu, D. Hu, Y. Kuang, B. Liu, X. Zhang, J. Chen, Functionalization of Carbon Nanotubes by an Ionic-Liquid Polymer: Dispersion of Pt and PtRu Nanoparticles on Carbon Nanotubes and Their Electrocatalytic Oxidation of Methanol, Angew. Chem. Int. Ed. 48 (2009) 4751–4754, https://doi.org/10.1002/anie.200900899.